UNITED NATIONS EDUCATIONAL, SCIENTIFIC AND CULTURAL ORGANIZATION
INTERNATIONAL ATOMIC ENERGY AGENCY
INTERNATIONAL CENTRE FOR THEORETICAL PHYSICS
I.C.T.P., P.O. BOX 586, 34100 TRIESTE, ITALY, CABLE: CENTRATOM TRIESTE

SMR.998c - 7

Research Workshop on Condensed Matter Physics
30 June - 22 August 1997
MINIWORKSHOP ON
PATTERN FORMATION AND SPATIO-TEMPORAL CHAOS
28 JULY - 8 AUGUST 1997

"Patterns and growth phenomena"

A. SANCHEZ
Universidad Carlos III de Madrid
Escuela Politecnica Superior
Departamento de Matematicas
c/Butarque 15
Leganes
28911 Madrid
SPAIN

These are preliminary lecture notes, intended only for distribution to participants.

Stochastic Model for Surface Erosion via Ion Sputtering: Dynamical Evolution from Ripple Morphology to Rough Morphology

Rodolfo Cuerno,[1] Hernán A. Makse,[1] Silvina Tomassone,[2] Stephen T. Harrington,[1] H. Eugene Stanley[1]
[1]*Center for Polymer Studies and Physics Department, Boston University, Boston, Massachusetts 02215*
[2]*Physics Department, Northeastern University, Boston, Massachusetts 02115*
(Received 25 July 1995)

Surfaces eroded by ion sputtering are sometimes observed to develop morphologies which are either ripple (periodic) or rough (nonperiodic). We introduce a discrete stochastic model that allows us to interpret these experimental observations within a unified framework. We find that a periodic ripple morphology characterizes the initial stages of the evolution, whereas the surface displays self-affine scaling in the later time regime. Further, we argue that the stochastic continuum equation describing the surface height is a noisy version of the Kuramoto-Sivashinsky equation.

PACS numbers: 68.35.Rh, 64.60.Ht, 79.20.Rf

A remarkable feature of erosion processes via ion sputtering in amorphous materials is the formation of a pattern consisting of a ripple structure, aligned in directions either parallel to or perpendicular to that of the bombarding beam of ions [1,2]. Indeed, we might expect that erosion tends to erase every possible feature of the surface morphology, and that the presence of noise in the system would further act against the formation of such a periodic pattern. Only recently have there been experimental [3] and theoretical [4] attempts to understand the formation of a ripple structure in the more general context of nonequilibrium interface growth phenomena [3]. Many such interfaces are "rough" and exhibit self-affine scaling at long distances and long times [1]; experimentally, one finds that surfaces eroded by ion bombardment *also* exhibit self-affine scaling behavior [5]. An outstanding question is then how to reconcile these observations with the formation of the periodic ripple structure.

In this Letter, we introduce a discrete stochastic model that incorporates the main physical mechanisms believed to influence the dynamics of the eroded surface morphology. We show that this model is characterized by an initial stage in which the surface morphology displays a ripple structure, and that subsequent stages are characterized by a crossover to a rough surface in the universality class of the Kardar-Parisi-Zhang (KPZ) equation [6]. We argue that the stochastic equation which provides the continuum description of our model is a *noisy* version [7] of the Kuramoto-Sivashinsky (KS) equation [8,9]. Thus we interpret the formation of a periodic pattern [3] and the development of rough interfaces [5] in the ion-sputtered systems as the early and late regimes, respectively, of the same dynamical process.

We first consider the main mechanisms [10] that determine the surface morphology undergoing ion bombardment.

(i) Erosion.—In ion sputtering, an initially flat substrate is bombarded with a well-collimated beam of heavy ions carrying a certain kinetic energy, and forming a precise angle with the normal to the uneroded surface. The phenomena leading to erosion take place within some finite distance from the surface. Namely, the ions penetrate inside the solid and induce along their path cascades of collisions among the atoms of the substrate. Atoms located at the surface may be affected by these collisions and acquire enough energy to leave the surface [11]. Consequently, atoms located at the bottom of troughs gain more energy on average and they are preferentially eroded as compared to those on the peaks of crests [12]. This "instability" can be thought of as a *negative surface tension*, since the surface tends to maximize its area.

(ii) Surface diffusion.—In physical systems there is a stabilizing mechanism that balances the negative surface tension, *surface diffusion*, which is always present at a nonzero temperature. Particles on the surface tend to diffuse looking for highly coordinated positions, a relevant phenomenon for sputtering [3,5] as well as for molecular-beam epitaxy (MBE) [13].

When the angle between the local normal to the surface and the incident beam approaches the grazing value, there is an increase in the reflection of the ions by the surface and the rate of erosion diminishes. This surface effect is beyond the approximations made in Sigmund's theory of ion sputtering [11], and is reflected in the angle

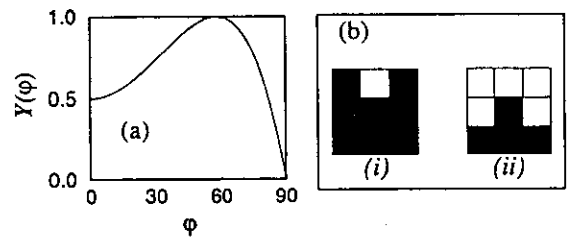

FIG. 1. (a) Sputtering yield $Y(\varphi)$ as a function of the angle φ. (b) Box rule for erosion. We define p_e as the number of occupied neighboring sites (grey squares) inside the 3×3 box centered at site i (black square), normalized by 7. The examples shown correspond to (i) $p_e = 1$ and (ii) $p_e = 3/7$.

 0031-9007/95/75(24)/4464(4)$06.00

dependence of the sputtering yield, $Y(\varphi)$, defined to be the number of eroded particles divided by the total number of bombarding ions. Here φ is the *local* angle of the ion trajectories to the surface normal at each point [14]. Typically [2], $Y(\varphi)$ is symmetric around $\varphi = 0$, presents a maximum between 60° and 80°, and decreases to zero as $\varphi \to 90°$.

To define the model, we introduce two dynamical rules, one to account for erosion and one to account for surface diffusion. The rule for erosion incorporates the unstable behavior described above as well as the phenomenological dependence of the sputtering yield as a function of φ. The model for the case of 1 + 1 dimensions [15] is defined on a square lattice of lateral size L, with periodic boundary conditions in the horizontal direction. The initial interface is a horizontal line separating occupied sites (below) from empty sites (above). We choose randomly a site i at the interface where $i = 1, \ldots, L$. The chosen site is subject to erosion with probability p, or to diffusion with probability $1 - p$, where the rules are as follows.

(i) Erosion (probability p).—[16] We compute $\varphi \equiv \tan^{-1}[(h_{i+1} - h_{i-1})/2]$, where h_i is the height of the interface at site i, and apply the erosion rule with probability $Y(\varphi)$, as given in Fig. 1(a). To erode, we count the number of occupied neighbors inside a square box of size 3×3 lattice spacings centered in the chosen site i (box rule). We empty the site with an erosion probability p_e proportional to the number of occupied cells in the box [see Fig. 1(b)]. Thus the box rule favors the erosion of troughs as compared to the peaks of crests, and therefore is the source of the instability in the ion-sputtered system.

(ii) Surface diffusion (probability $1 - p$).—A diffusive move of the particle i to a nearest neighbor column is attempted with hopping probability $w_{i \to f} \equiv [1 + \exp(\Delta \mathcal{H}_{i \to f}/k_B T)]^{-1}$, where $\Delta \mathcal{H}_{i \to f}$ is the energy difference between the final and initial states of the move. Following [17], we choose $\mathcal{H} \equiv (J/2) \sum_{\langle i,j \rangle} (h_i - h_j)^2$.

A continuum equation that describes the dynamics of the interface height has the form

$$\partial_t h(x,t) = \nu \nabla^2 h - \kappa \nabla^4 h + \eta(x,t) + f_Y[h(x,t)]. \tag{1}$$

Here $h(x,t)$ is the height of the interface at position x and time t, ν is a negative surface tension coefficient, κ is a positive coefficient that accounts for the surface diffusion, and $\eta(x,t)$ is a Gaussian noise term with short range correlations and strength $2D$ that accounts for the fluctuations in the flux of incoming particles. The functional $f_Y[h]$ takes into account the contribution of nonlinear terms, which appear in the equation of motion due to the effect of $Y(\varphi)$, itself a nonlinear function of the local slope $\nabla h \equiv \tan \varphi$. The nonlinearities become more relevant in the equation of motion at the late regime of the evolution when large slopes develop (see below).

First we study the model in the case $Y(\varphi) \equiv 1$, which approximately holds at the early stages of evolution. We focus on the time dependence of the total interface width $W(t) \equiv \langle L^{-1} \sum_{i=1}^{L} [h_i(t) - \overline{h(t)}]^2 \rangle^{1/2}$, where $\overline{h(t)} \equiv L^{-1} \sum_{i=1}^{L} h_i(t)$, and the brackets denote an average over realizations of the noise. The erosion rule alone—corresponding to $p = 1$, $Y(\varphi) \equiv 1$—leads to $W(t) \sim t$, which can be attributed to ν in (1) being a negative number [18]. Moreover, by considering only the erosion rule, but defined with probability $1 - p_e$, we find that the interface has the scaling properties of the Edwards-Wilkinson (EW) equation [19] that is obtained from (1) with $\nu > 0$, $\kappa = 0$, and $f_Y[h] = 0$. We understand this result since one favors the erosion of

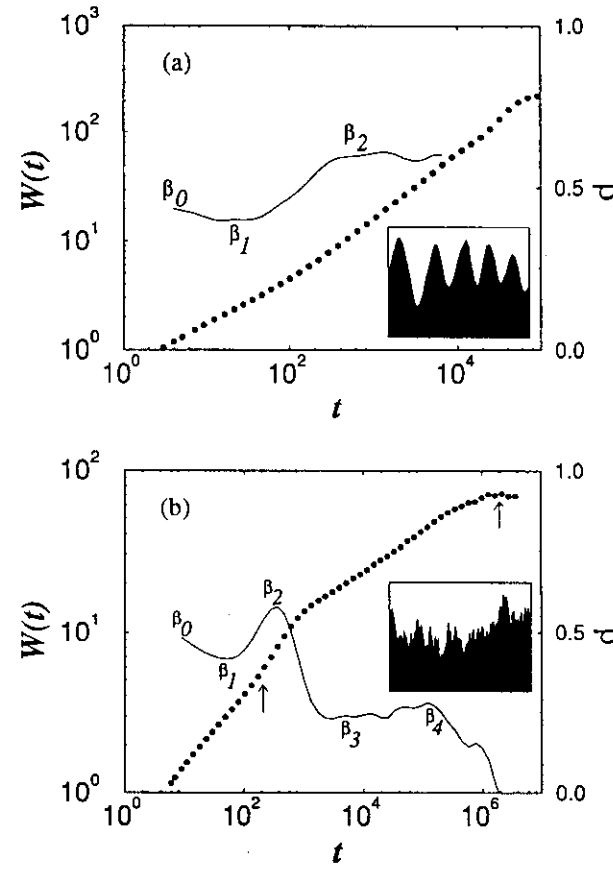

FIG. 2. Time evolution of the surface width for the cases $Y(\varphi) \equiv 1$ and $L = 50$. The solid line is the consecutive slope of the width, showing the value of the growth exponent β in each regime. The inset shows the ripple structure of the interface at $t = 1000$. The saturation observed in $W(t)$ is due to the discreteness of the lattice: the erosion rule breaks down when the local slopes of the interface are bigger than 3 [20]. This effect can be avoided by using a bigger box. (b) Interface width as a function of time for the full model showing the regimes of the evolution for $L = 2048$. As in (a), the solid line is the consecutive slope. The inset shows a portion of the rough morphology at the late regime, where the self-affine scaling behavior holds. The arrows indicate the times at which the structure factor is displayed in Fig. 3.

peaks as compared to valleys, leading to the smoothing mechanism characteristic of a positive surface tension. On the other hand, the surface diffusion mechanism alone [for $p = 0, Y(\varphi) \equiv 1$] is well described by (1) with $\nu = 0$, $\kappa > 0$, and $f_Y[h] = 0$, i.e., the linear MBE equation [13,17]. When mechanisms (i) and (ii) above are considered simultaneously for $J/k_BT = 5$, $p = 0.5$, and $Y(\varphi) \equiv 1$, we obtain the different stages of the time evolution displayed in Fig. 2(a) [21]. There exists a first region [22] for which $W(t) \sim t^{\beta_1}$, with $\beta_1 = 0.38 \pm 0.02$, the growth exponent for the linear MBE universality class, after which $W(t)$ scales with $\beta_2 > 0.5$ due to the instability caused by $\nu < 0$. In this case, a linear stability analysis of (1) shows that there is a maximally unstable mode in the system, $k_m = (|\nu|/2\kappa)^{1/2}$, and therefore the surface is almost periodic [inset in Fig. 2(a)].

Next we consider the model with $Y(\varphi)$ shown in Fig. 1(a). The results are not expected to depend strongly on the specific form of $Y(\varphi)$, so long as it preserves the existence of a maximum, and $Y(0) \neq 0$, $Y(90°) = 0$ [23]. Figure 3 shows the structure factor $S(k) \equiv \langle \hat{h}(k,t)\hat{h}(-k,t)\rangle$ at the onset of the instability. Here $\hat{h}(k,t)$ is the Fourier transform of $h_i(t) - \overline{h(t)}$. As we see, the early stages of the dynamics are still dominated by the periodic ripple structure defined by the competition between surface tension and surface diffusion, described by the linear part of (1).

For later times, the large slopes built up by the instability induce nonlinear effects, and the interface results in a rough morphology [inset of Fig. 2(b)]. In Fig. 2(b), we present the time evolution of $W(t)$ for the complete model. We again observe a first regime [22] with $\beta_1 = 0.38 \pm 0.03$, followed by unstable erosion ($\beta_2 > 0.5$). For later stages, we find $\beta_3 = 0.23 \pm 0.03$, consistent with EW, after which a crossover to $\beta_4 = 0.28 \pm 0.03$ is found. Finally, the width saturates due to the finite size of the system. Note that the value of the growth exponent for the KPZ equation is $\beta_{KPZ} = 1/3$ [6]. At saturation, $S(k)$ displays the small momenta behavior $S(k,t) \sim k^{-2}$, consistent with the scaling of both the EW and KPZ universality classes (see Fig. 3). To determine if a KPZ nonlinearity is present in Eq. (1), we compute the mean velocity $v(m)$ of the interface in the saturated regime as a function of an average tilt $m \equiv \langle \nabla h \rangle$ imposed by using helical boundary conditions. If we assume that the relevant nonlinearity in (1) is of the KPZ type, then $f_Y[h] = (\lambda/2)(\nabla h)^2$. Taking spatial and noise averages in (1), $v = v_0 + (\lambda/2)m^2$, where v_0 is the velocity of the untilted interface [24]. The parabolic shape of $v(m)$ obtained in our simulations (see Fig. 4) leads to the conclusion that the long time and long distance behavior of the model falls into the KPZ universality class. Moreover, the continuum equation describing the model ion-sputtered surfaces is the *noisy* KS equation

$$\partial_t h = \nu\nabla^2 h - \kappa\nabla^4 h + \frac{\lambda}{2}(\nabla h)^2 + \eta(x,t). \qquad (2)$$

To compare the *dynamics* of (2) with those obtained for the discrete model, we integrate numerically Eq. (2) in 1 + 1 dimensions. Figure 5 shows the behavior of the function $W(t)$. We observe the same crossovers as in the model [22]: $\beta_1 = 0.38 \pm 0.03$ corresponding to the linear MBE case, followed by unstable growth $\beta_2 > 0.5$. Then, a transition to EW behavior $\beta_3 = 0.25 \pm 0.03$ is observed, after which the nonlinearities dominate and a KPZ growth with $\beta_4 = 0.30 \pm 0.03$ is obtained. Finally, the interface width saturates due to the finite size of the system. Consistent with these numerical findings, the late scaling of Eq. (2) has been shown through a renormalization-group calculation [7] to be that of the KPZ equation in 1 + 1 and 2 + 1 dimensions. As we see, both in the model and the *noisy* KS, there is a long crossover time from EW to KPZ behavior, responsible for the difference between β_4 and β_{KPZ}, and for the narrow

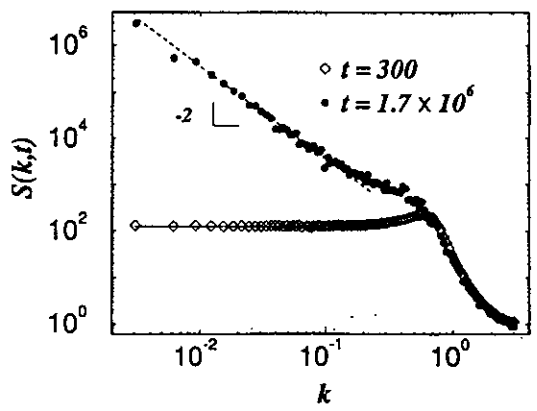

FIG. 3. Structure factor computed using the full model for a system with $L = 2048$. For $t = 300$, averaged over 2600 noise realizations (◇), and for $t = 1.7 \times 10^6$, averaged over 39 realizations (•) [see arrows in Fig. 2(b)]. The solid line is a fit by the exact solution of the discretized linear part of Eq. (1). The dashed straight line has slope −2.

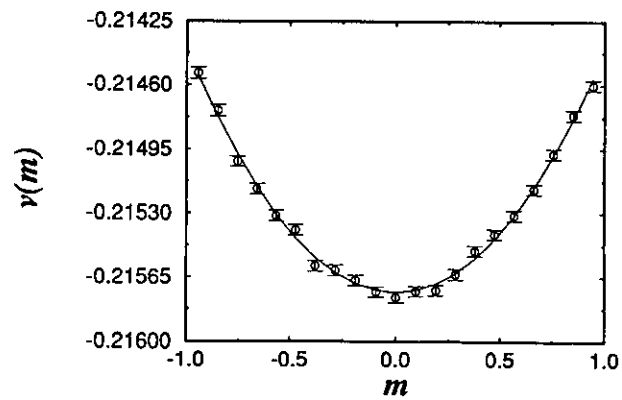

FIG. 4. Plot of the mean velocity $v(m)$ as a function of the average tilt m of the interface, calculated in the saturated regime for $L = 128$, and averaged over 810 noise realizations. The solid line is a fit to a parabola.

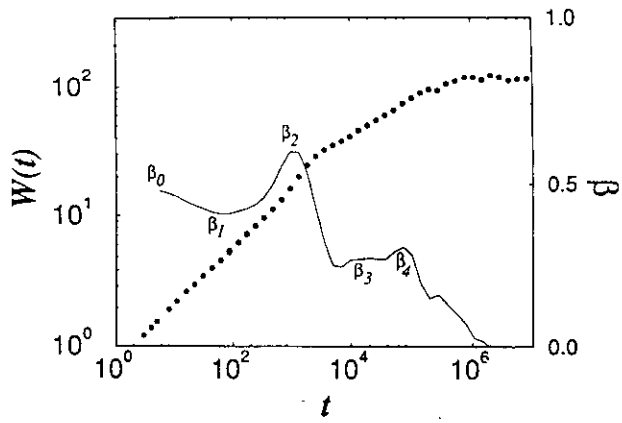

FIG. 5. Log-log plot of the interface width as a function of time obtained in the numerical integration of Eq. (2). The mesh is $\Delta x = 1.0$ and the time step $\Delta t = 0.005$. Parameter values are $\nu = -1$, $\kappa = 1$, $\lambda = 4$, $D = 0.5$, and $L = 1024$. The solid line gives the consecutive slopes.

window in which β_4 is observed—we find that the width of this window increases systematically with L. A similar phenomenon is well known to occur in the *deterministic* KS equation in 1 + 1 dimensions (see Sneppen *et al.* [9].

Finally, we compare the results of the model with observations of recent experiments [25]. The experimental development of a ripple structure [3] is well understood in terms of the unstable linear theory of ion sputtering describing the early stages of the time evolution of the model presented here. Moreover, the model predicts that in the late regime the large slopes generated by the unstable growth trigger the action of nonlinearities which stabilize the surface. The nonlinearity we find is of the KPZ type, consistent with the experimental observation of KPZ scaling reported by Eklund *et al.* [5]. To confirm the above picture, it would be of interest to study experimentally if both regimes do effectively take place in the time evolution of the *same* physical system.

We acknowledge discussions with A. L. Barabási, G. Carter, S. Havlin, and K. B. Lauritsen. R. C. acknowledges support from Ministerio de Educación y Ciencia, Spain. The Center for Polymer Studies is funded by NSF.

[1] P. Meakin, Phys. Rep. **235**, 189 (1993); T. Halpin-Healey and Y.-C. Zhang, *ibid.* **254**, 215 (1995); A.-L. Barabási and H. E. Stanley, *Fractal Concepts in Surface Growth* (Cambridge University Press, Cambridge, 1995).

[2] G. Carter *et al.*, in *Sputtering by Particle Bombardment*, edited by R. Behrisch (Springer-Verlag, Heidelberg, 1983), Vol. II, p. 231.

[3] E. Chason *et al.*, Phys. Rev. Lett. **72**, 3040 (1994); T. M. Mayer *et al.*, J. Appl. Phys. **76**, 1633 (1994).

[4] R. Cuerno and A. L. Barabási, Phys. Rev. Lett. **74**, 4746 (1995).

[5] E. A. Eklund *et al.*, Phys. Rev. Lett. **67**, 1759 (1991); E. A. Eklund *et al.*, Surf. Sci. **285**, 157 (1993); J. Krim *et al.*, Phys. Rev. Lett. **70**, 57 (1993); H.-N. Yang, G.-C. Wang, and T.-M. Lu, Phys. Rev. B **50**, 7635 (1994).

[6] M. Kardar, G. Parisi, and Y.-C. Zhang, Phys. Rev. Lett. **56**, 889 (1986).

[7] R. Cuerno and K. Lauritsen, Phys. Rev. E **52**, 4853 (1995). For $d > 2$, see L. Golubović and R. Bruinsma, Phys. Rev. Lett. **66**, 321 (1991); **67**, 2747(E) (1991).

[8] Y. Kuramoto and T. Tsuzuki, Prog. Theor. Phys. **55**, 356 (1977); G. I. Sivashinsky, Acta Astronaut. **6**, 569 (1979).

[9] S. Zaleski, Physica (Amsterdam) **34D**, 427 (1989); K. Sneppen *et al.*, Phys. Rev. A **46**, R7351 (1992); F. Hayot *et al.*, Phys. Rev. E **47**, 911 (1993).

[10] Here we neglect redeposition of the eroded material, as well as shadowing effects among different surface features. These assumptions have been shown [3] to hold at the initial stages of surface evolution. The roughening taking place in the model at late time stages is again consistent with them.

[11] P. Sigmund, Phys. Rev. **184**, 383 (1969).

[12] P. Sigmund, J. Mater. Sci. **8**, 1545 (1973); R. M. Bradley and J. M. E. Harper, J. Vac. Sci. Technol. A **6**, 2390 (1988).

[13] C. Herring, J. Appl. Phys. **21**, 301 (1950); W. W. Mullins, J. Appl. Phys. **28**, 333 (1957); in the context of stochastic models, see D. E. Wolf and J. Villain, Europhys. Lett. **13**, 389 (1990); S. Das Sarma and P. I. Tamborenea, Phys. Rev. Lett. **66**, 325 (1991).

[14] When we fix the type of bombarding ion, the material of the substrate, and the energy of the incoming beam, $Y(\varphi)$ is a function of φ only.

[15] The generalization to 2 + 1 dimensions will be reported elsewhere.

[16] We consider normal incidence of the ions onto the substrate.

[17] M. Siegert and M. Plischke, Phys. Rev. E **50**, 917 (1994).

[18] Strictly speaking, $\nu < 0$ implies exponential growth for W, which cannot be attained in the present definition of the box rule, since at most only L particles can be eroded per unit time, leading to $W \sim t$ as the fastest growth for the width.

[19] S. F. Edwards and D. R. Wilkinson, Proc. R. Soc. London A **381**, 17 (1982).

[20] K. Lauritsen (private communication).

[21] Qualitatively the results do not change when other values of J/k_BT and p are considered.

[22] An initial random erosion regime ($\beta_0 = 0.5$) is also observed before correlations build up in the system.

[23] G. Carter *et al.*, Surf. Interface Anal. **20**, 90 (1993); A. N. Protsenko, Nucl. Instrum. Methods Phys. Res., Sect. B **82**, 417 (1993).

[24] J. Krug and H. Spohn, Phys. Rev. Lett. **64**, 2332 (1990).

[25] Based on our identification of Eq. (2) as describing the model, and the scaling of this equation in 2 + 1 dimensions predicted in [7], we expect our results to carry over for the physical case of two-dimensional surfaces. An important ingredient in 2 + 1 dimensions is the anisotropy between the two substrate directions induced by the ion beam. This leads to effects such as the change in the orientation of the ripples as a function of the angle of incidence [12], and could be accounted for by introducing a non-zero angle of incidence.

DEPARTAMENTO DE MATEMÁTICAS
ESCUELA POLITÉCNICA SUPERIOR

GRUPO INTERDISCIPLINAR DE
SISTEMAS COMPLICADOS

UNIVERSIDAD CARLOS III DE MADRID
c/Butarque, 15 28911 – Leganés

Patterns and Growth Phenomena

Collaborators: Esteban Moro

Rodolfo Cuerno U. Carlos III

Alan Bishop Los Alamos Lab

Hilda Cerdeira ICTP, Trieste

What are patterns?

M. C. Cross, P. C. Hohenberg Rev. Mod. Phys. 65, 851 (1993)

- Unified description based on linear instabilities of homogeneous sta
- Characteristic wavevector q_0 and frequency ω_0
  - I_s : $\omega_0 = 0$, $q_0 \neq 0$
  - III_0 : $\omega_0 \neq 0$, $q_0 = 0$
  - I_0 : $\omega_0 \neq 0$, $q_0 \neq 0$
- Relationship of patterns and spatio-temporal chaos
  - Low dimensional chaos
  - Order and disorder in spatial patterns

More on patterns:

Patterns: Formation and Competition.

(Excerpt from D. Campbell, "Introduction to Nonlinear Phenomena," in "Lectures in the Sciences of Complexity", Addison-Wesley, 1990)

When a spatially extended nonlinear system is driven far from equilibrium, the many localized coherent structures that typically arise can organize themselves into a bewildering array of spatial patterns, regular or random. Perhaps the most familiar example is turbulent fluid flow, in which the temporal behavior is chaotic yet one frequently observes patterns of coherent structures. (...) A typical, extended, nonlinear nonequilibrium system will have many possible configurations or patterns; some of these will be stable, others unstable, and the vast majority metastable. Highly symmetric patterns may be accessible analytically, but general, anisotropic configurations must first be studied via experimental mathematics. (...) The interplay between coherent structures and temporal chaos can give rise to a myriad of patterns, which typically form and compete on a continuous basis.

Aim: Present (a few) examples of "pattern issues" arising from growth phenomena and models

- Ion sputtering:
  - Periodic patterns vs chaos
  - Noisy Kuramoto-Sivashinsky equation
- Epitaxial growth:
  - Collective locking
  - Random patterns
  - Noisy nonlinear diffusion equations

Ion sputtering :

Old technique (~125 years!)

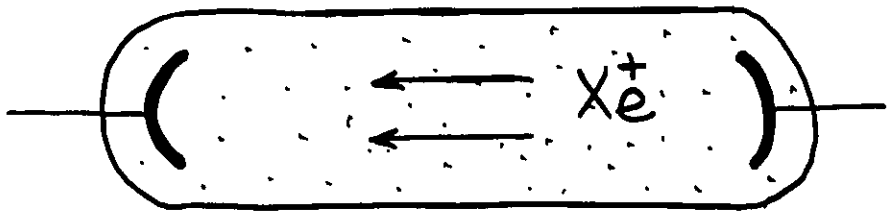

Many applications :

polishing, cleaning
thin film deposition
controlled removal

Experimental setup :

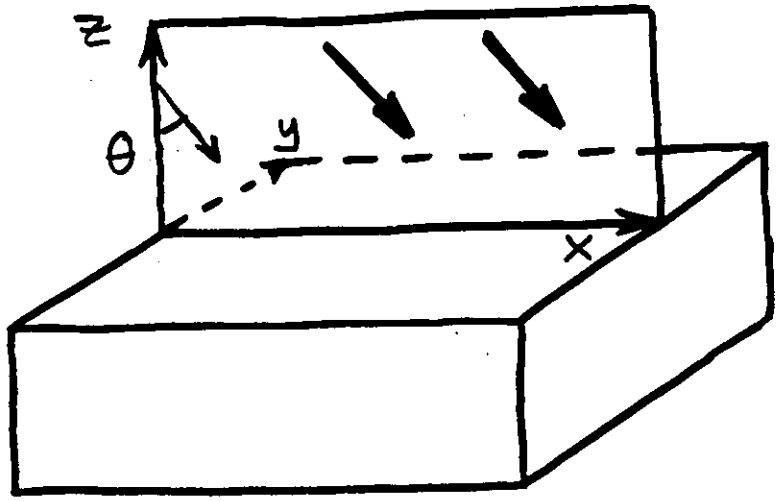

Chason et al. JAP (94)

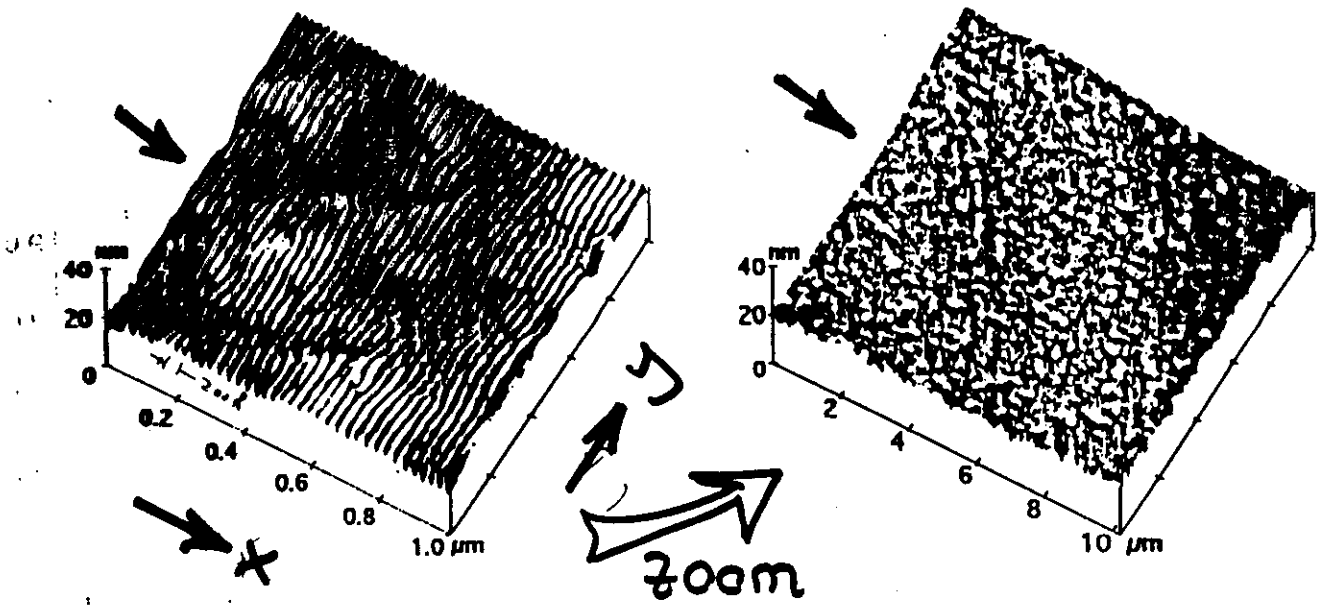

SiO_2

1 keV Xe^+ „ $\theta \sim 55°$

Graphite

5 keV Ar^+ „ $\theta \sim 60°$

Eklund et al.

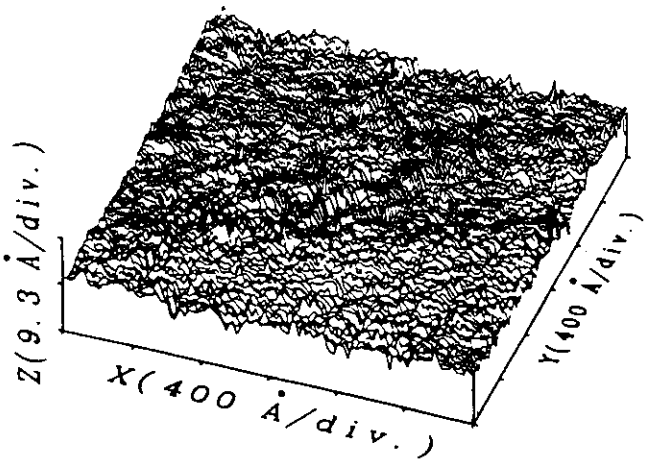

FIG. 1. Constant-current STM topograph of a graphite surface after sputtering with a flux J of 6.9×10^{13} ions/cm^{2}sec and an ion fluence Q of 10^{16} ions/cm^2 at room temperature. The X and Y dimensions are 2400 Å and the total Z dimension is 18.6 Å.

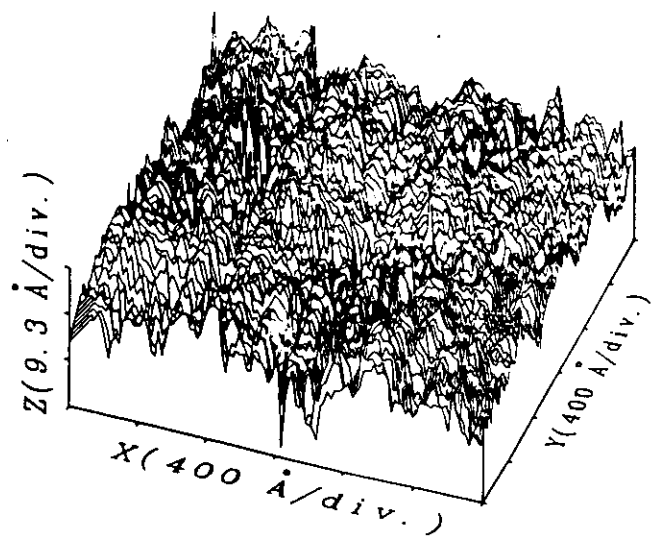

FIG. 2. STM topograph with the same parameters as that in Fig. 1, except that $Q = 10^{17}$ ions/cm^2 and the total Z scale is 27.9 Å.

Modelo discreto

(R.C., Makse, Toussaint, Harrington, Stanley)

Inicialmente:

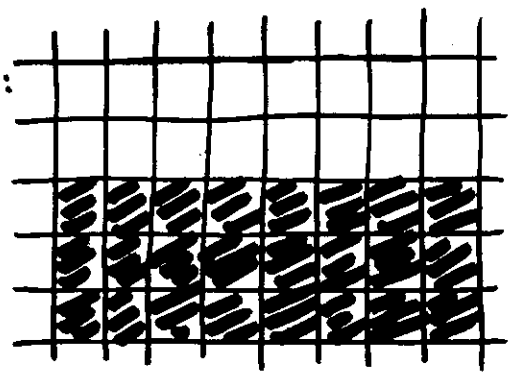

2 reglas ⇝ (tasa relativa p)

i) Erosión (p):

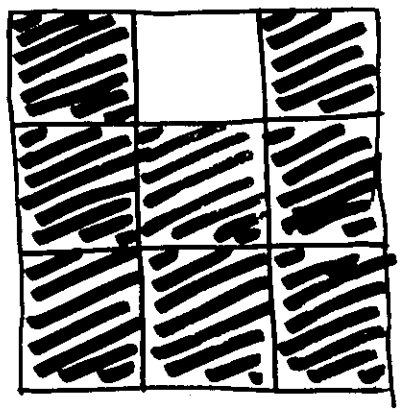

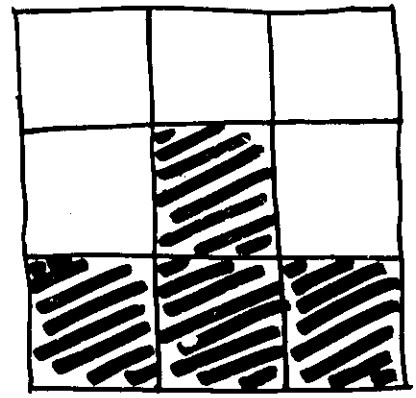

$p_e = \frac{7}{7} = 1$

$p_e = 3/7$

Inestabilidad

Efectividad

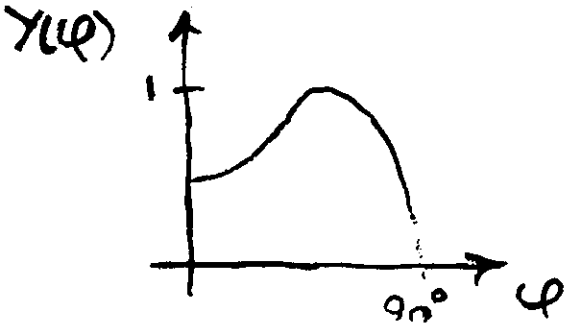

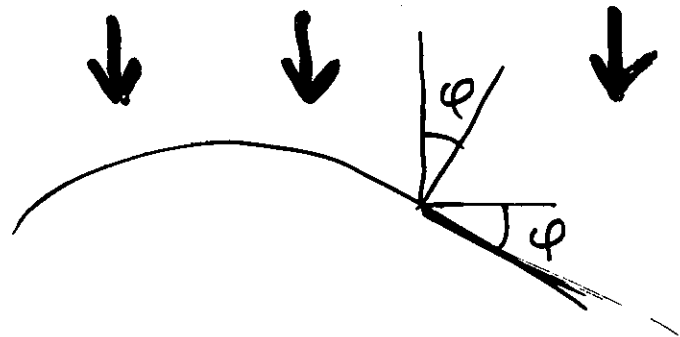

ii) Difusion a lo largo de la superficie $(1-p)$

$$\omega_{i\to f} = \frac{1}{1 + e^{\beta \Delta H_{i\to f}}}$$

$$\Delta H_{i\to f} = H_{final} - H_{inicial} \quad ,, \quad H = J \sum_{i=1}^{L} (h_i - h_{i+1}$$

MBE Siegert y Plischke

El modelo evoluciona según

$$\frac{\partial h}{\partial t} = -|v| \partial_x^2 h + \frac{\lambda}{2} (\partial_x h)^2 - K \cdot \partial_x^4 h + \eta(x,$$

Kuramoto - Sivashinsky ⇝

⇝ Caos espaciotemporal

evolución temporal:

estructura simple (inestabilidad) ⇝ superficie rugosa (KPZ)

Dynamic scaling (brief detour):

ROUGH surfaces are ubiquitous

Characterisation:

Mean height: $\bar{h}(t) \equiv \frac{1}{L} \sum_{i=1}^{L} h_i(t)$

WIDTH (rms): $w^2(L,t) \equiv \left\langle \frac{1}{L} \sum_{i=1}^{L} \left(h_i(t) - \bar{h}(t) \right)^2 \right\rangle$

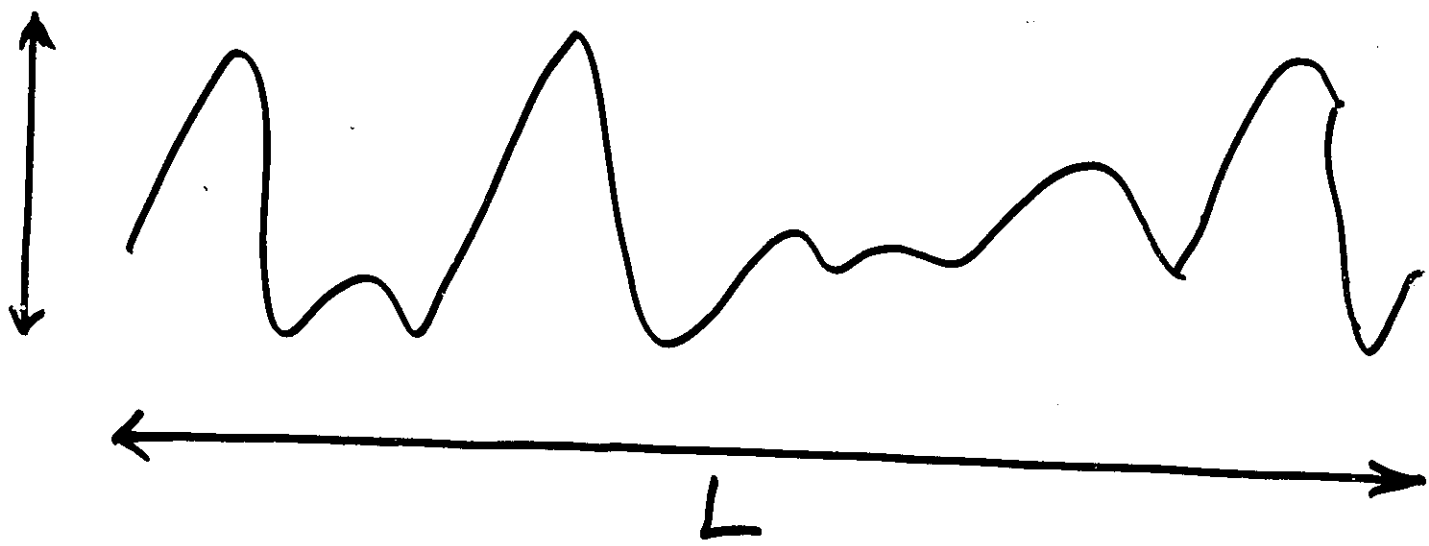

Observations:

$$w(L,t) \sim t^{\beta} \quad , \quad t \ll t_x$$

$$w_{sat}(L) \sim L^{\alpha} \quad , \quad t \gg t_x$$

$$t_x \sim L^{z}$$

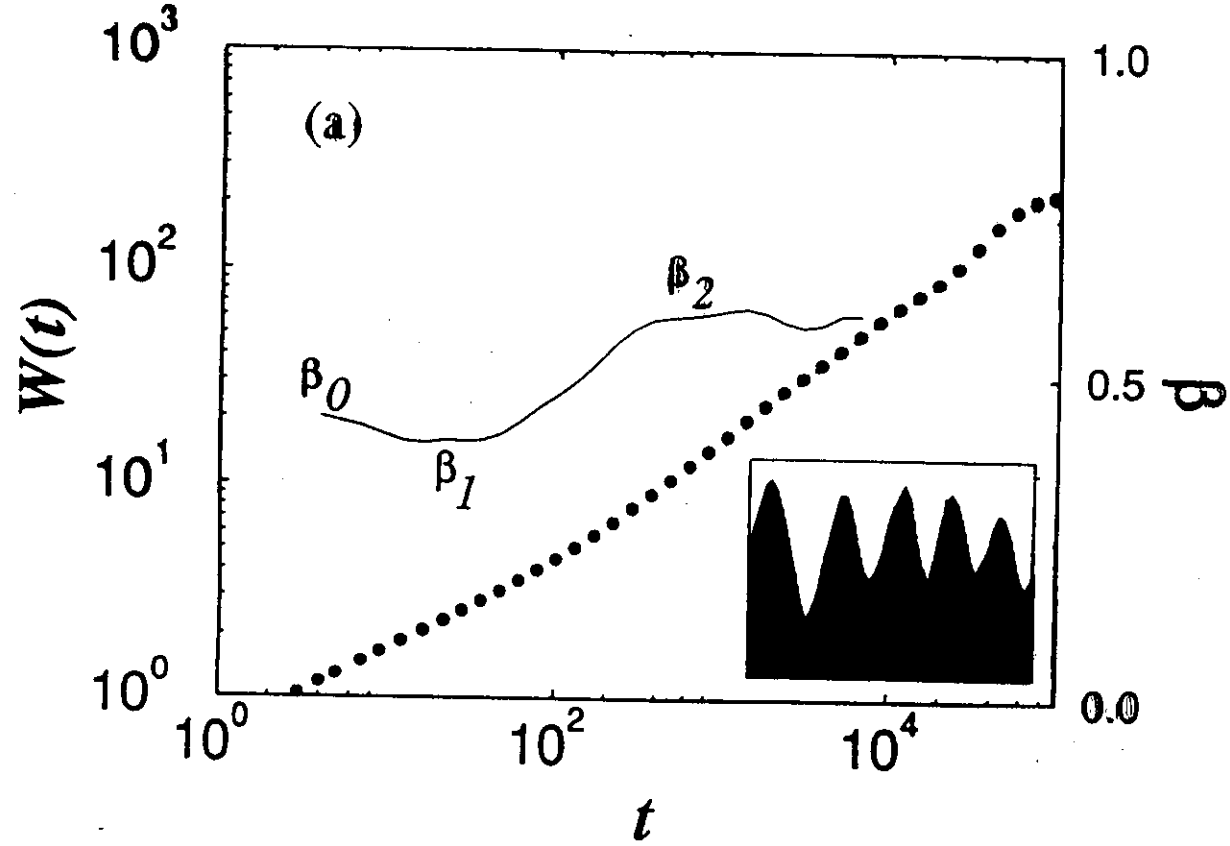
(a)
10^3
10^2
10^1
10^0
W(t)
1.0
0.5
0.0
β
$β_0$
$β_1$
$β_2$
10^0
10^2
10^4
t

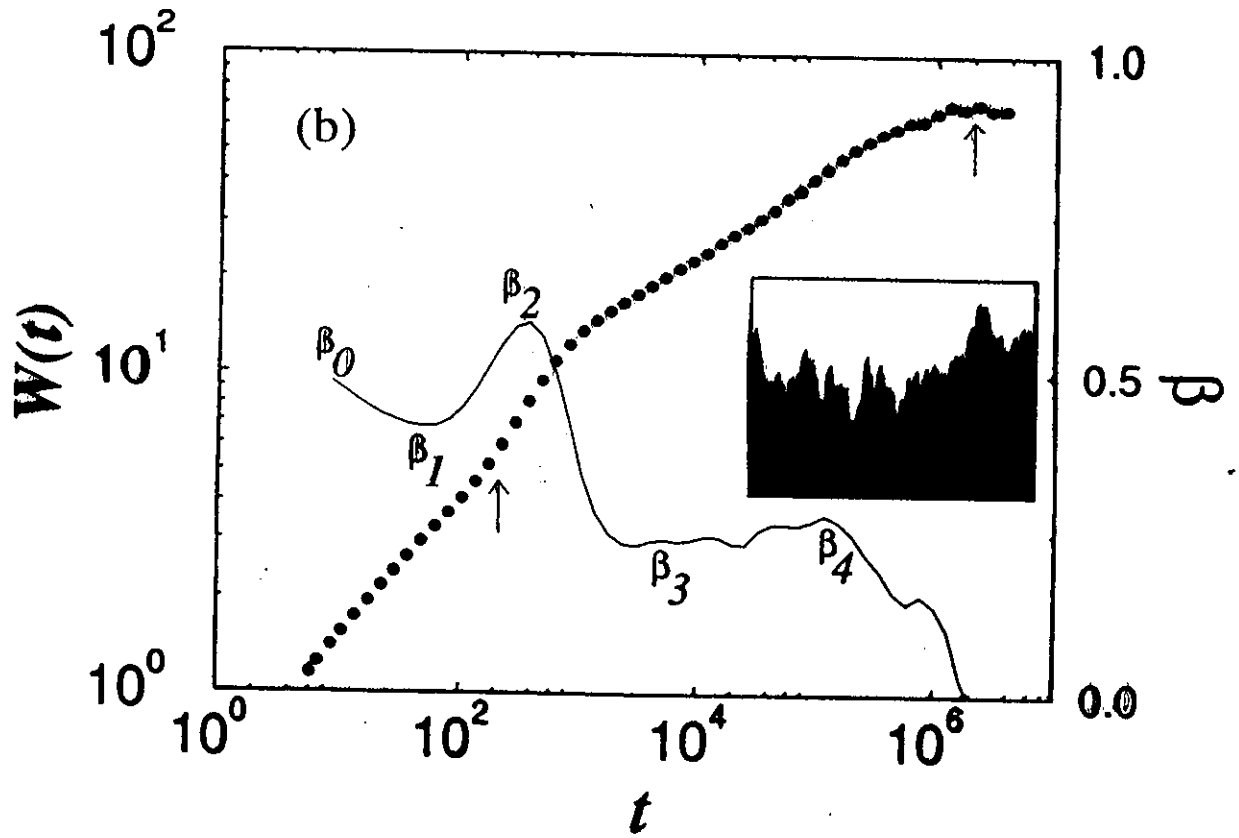
(b)
10^2
10^1
10^0
W(t)
1.0
0.5
0.0
β
$β_0$
$β_1$
$β_2$
$β_3$
$β_4$
10^0
10^2
10^4
10^6
t

Inicialmente

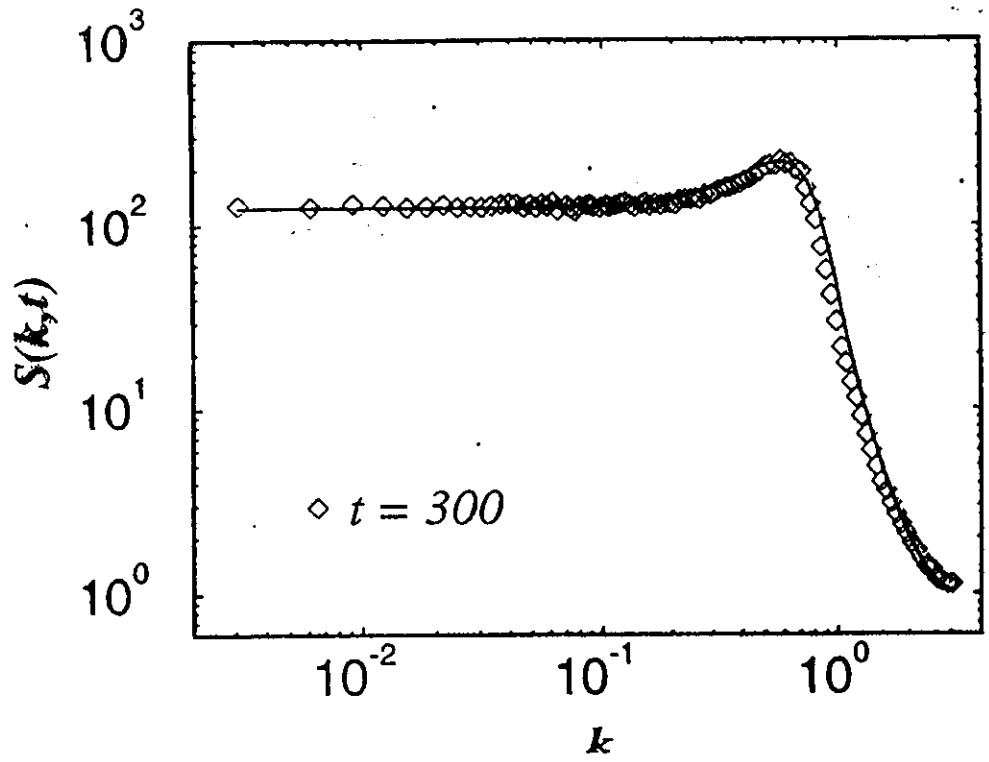

◇ modelo

— solución exacta ecuación lineal

↓

~ Chasan et al.

Etapas tardías

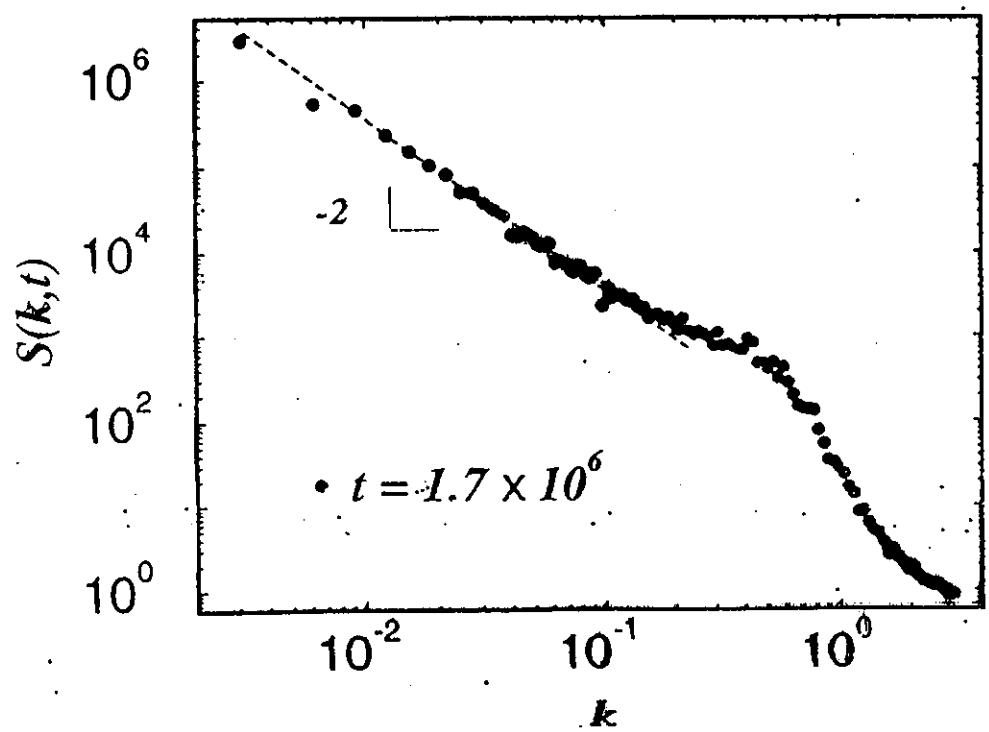

→ $\alpha = 1/2$ consistente con KPZ

~ Ekland et al.

Physical considerations:

* Symmetry:

$x \longrightarrow -x$ NOT

$y \longrightarrow -y$ O.K.

* Surface tension:

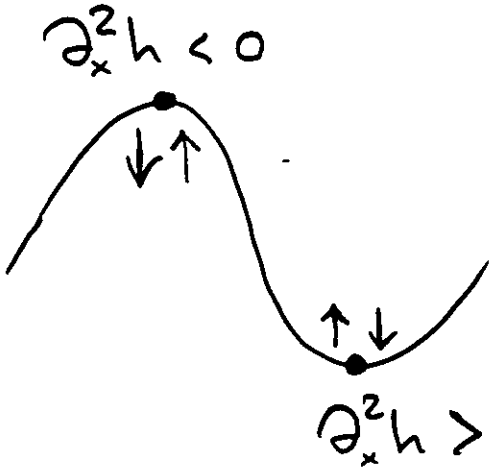

$$\partial_t h = \nu \partial_x^2 h$$

$\nu > 0$ smoothing

$\nu < 0$ unstable!

* Lateral motion:

$$\partial_t h = \frac{\lambda}{2} (\partial_x h)^2$$

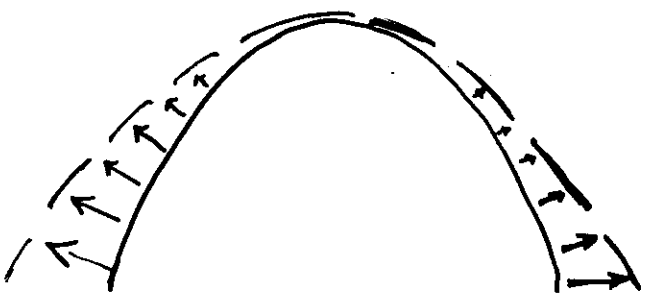

Lateral motion along normal

Kardar, Parisi, Zhang

Additional physical mechanisms:

* Surface diffusion:

  Curvature driven

  Thermally activated

$$\frac{\partial h}{\partial t} + \nabla \cdot \vec{J} = 0 \quad , \quad \vec{J} = -\nabla \mu$$

$\mu \propto -$ curvature

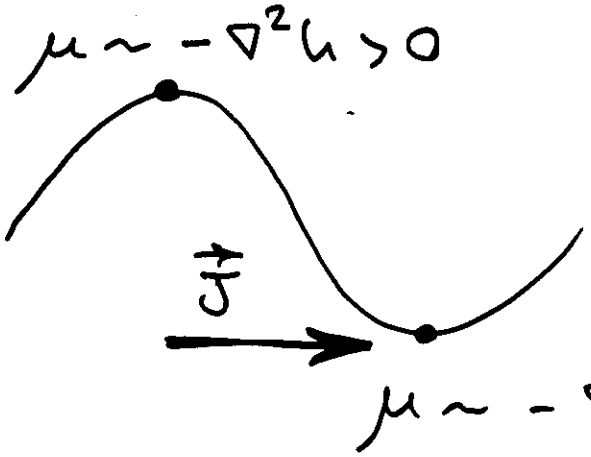

$$\frac{\partial h}{\partial t} = -K \nabla^2 (\nabla^2 h$$

$K > 0$

* Fluctuations in the beam:
  (→ ROUGHNESS)

$$\langle \eta(\vec{x},t)\, \eta(\vec{x}',t') \rangle = 2D\, \delta^{(2)}(\vec{x}-\vec{x}')\, \delta(t-t'$$

$$D^{1/2} \propto \Phi$$

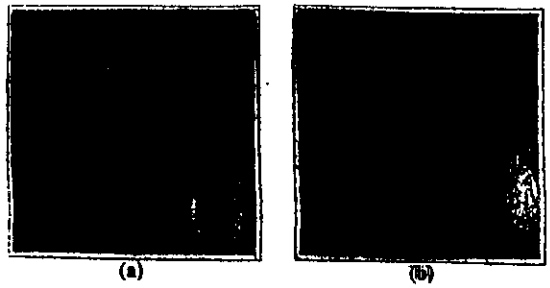

Rost, Krug PRL 1995

FIG. 2. Gray level plot of two snapshots of a system of size 50×50 with $\alpha = -1$ and isotropic nonlinearity ($\beta = 1$). The left picture was taken at an early time, before the nonlinearity becomes relevant (the amplitude still being small). The right shows the same system at a later time, in the chaotic regime. The ripples pinch off.

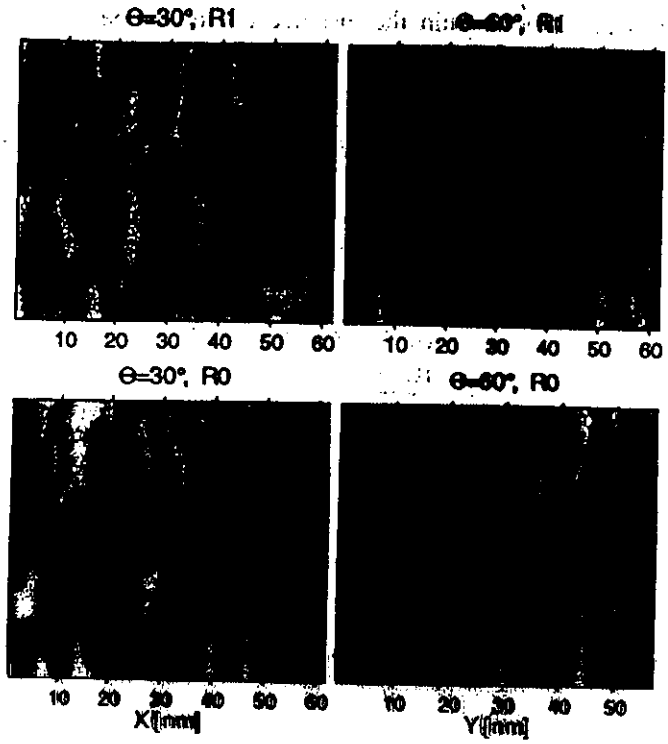

Koponen et al 1997

FIG. 4. The effect of diffusion on the ripple formation. The angle of incidence and the model of surface relaxation are denoted. The fluences corresponding to the situation shown are for model R1 approximately 2×10^{17} ions/cm^2 and for model R0 5×10^{16} ions/cm^2. Otherwise similar to Fig. 1.

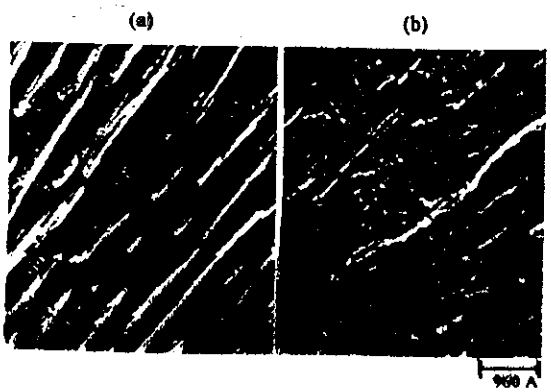

Flosdorf et al. 1997

FIG. 4. Two images acquired at $T_0 = 200$ K after sputtering at equal fluence (10.5 ML) but at different ion fluxes, 0.035 ML sec^{-1} (a) and 0.01 ML sec^{-1} (b), respectively. $T_S = 300$ K and $E_i = 1$ keV.

Microscopic processes involved

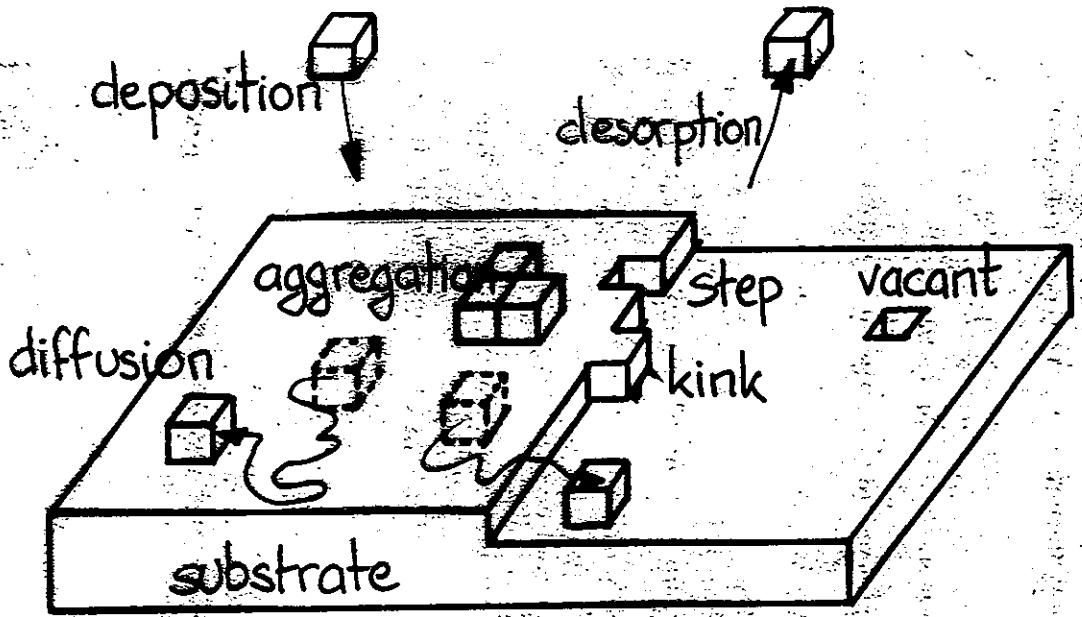

Very general description:
applicable to other problems
in physics and elsewhere

Dates back to 1951:
Burton, Cabrera, Frank

Related growth techniques

- Vapor phase
  - MBE
  - CVD, MOCVD
  - ALE
- Liquid phase
  - From the melt
  - From solutions
  - Electrodeposition

Deposición de Si en fase gaseosa

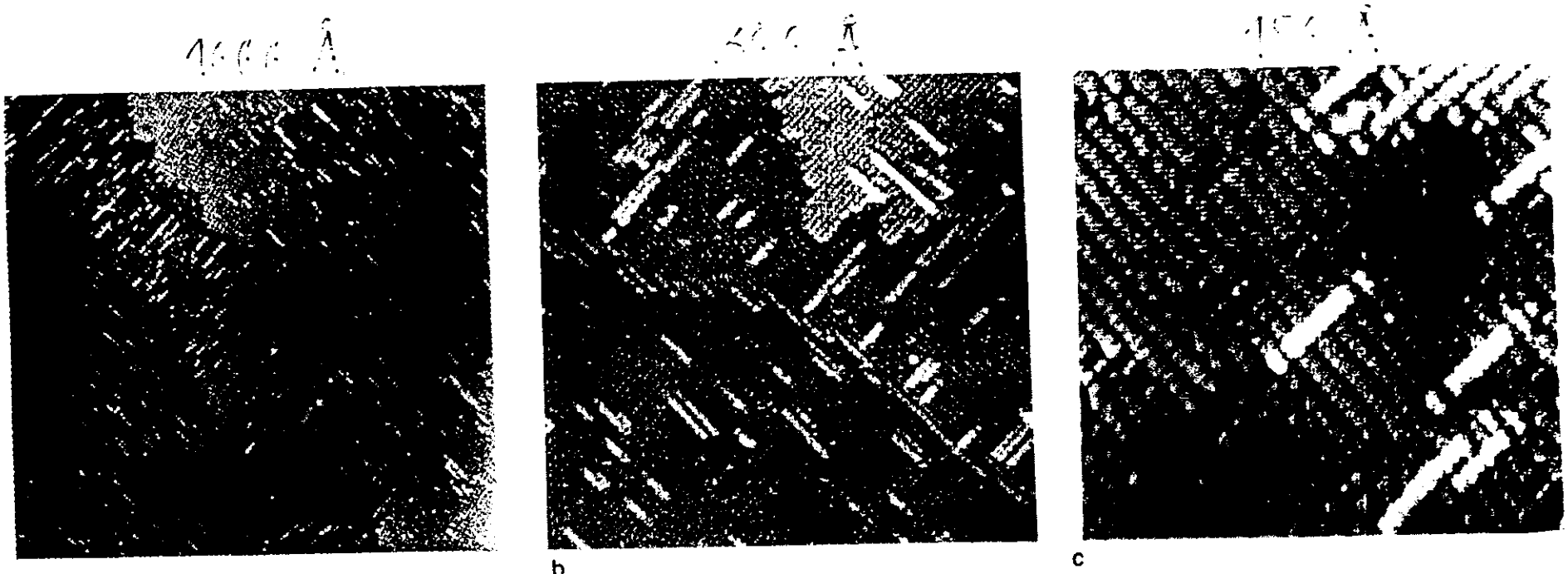

Growth of two-dimensional silicon islands. on a Si(001) surface, observed at various magnifications with a scanning tunneling microscope. In all the images, brighter regions are higher. **a:** At low magnification (with a field of

[M.G. Lagally, Phys. Today November '93, 27]

- Distintos regímenes de crecimiento
- Distintos niveles de descripción
- Auto-afinidad

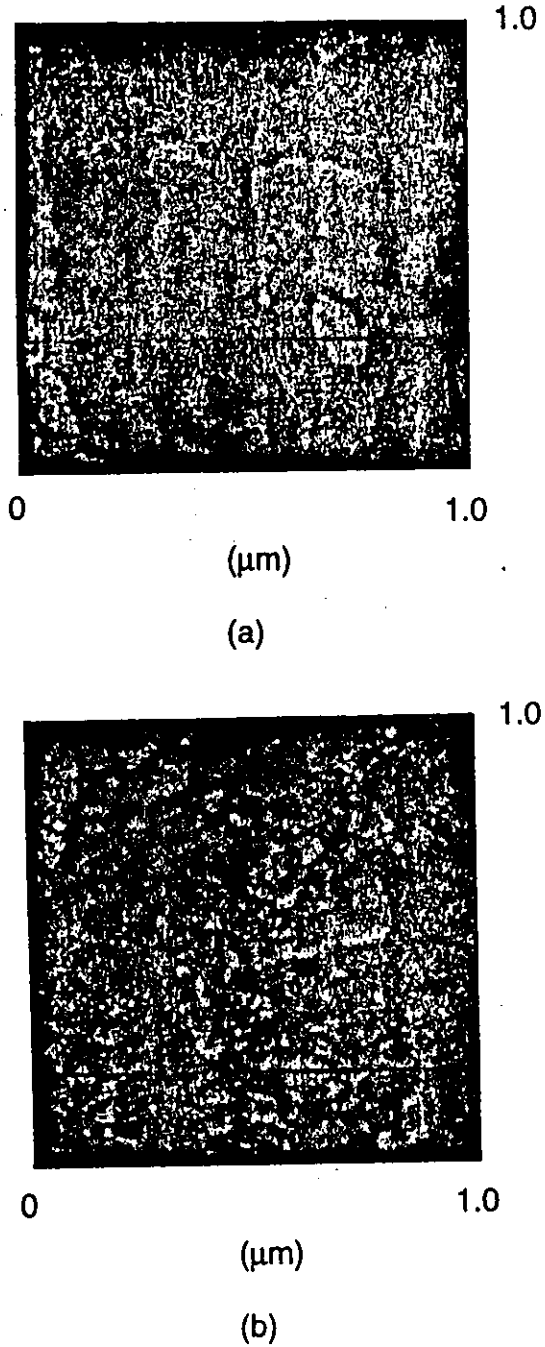

FIG. 1. Atomic force microscope images of GaInP layers grown on singular (001) GaAs substrates at 670 °C at growth rates of (a) 0.25 and (b) 2.0 μm/h. The solid lines are in the [1̄10] direction.

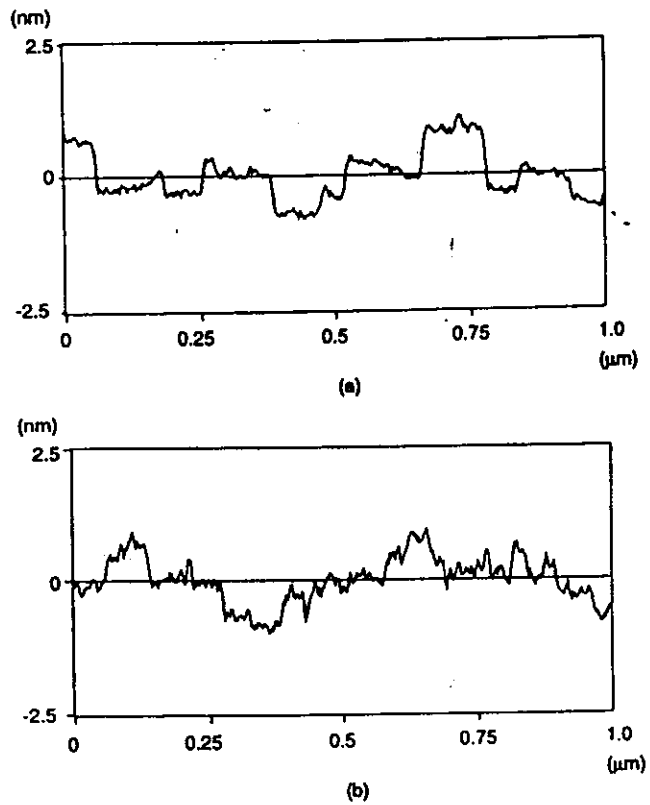

FIG. 2. Atomic-scale profiles of the surfaces of the GaInP samples shown in Fig. 1; (a) 0.25, (b) 2.0 μm/h taken along the solid lines in Fig. 1.

Chin, Lee, Ho & Stringfellow
J Appl Phys 81, 646 (1997)

Two Main Classes of Models:

- (Nonlinear) Stochastic **PDE**s e.g. KPZ, EW
- Discrete **M**odels

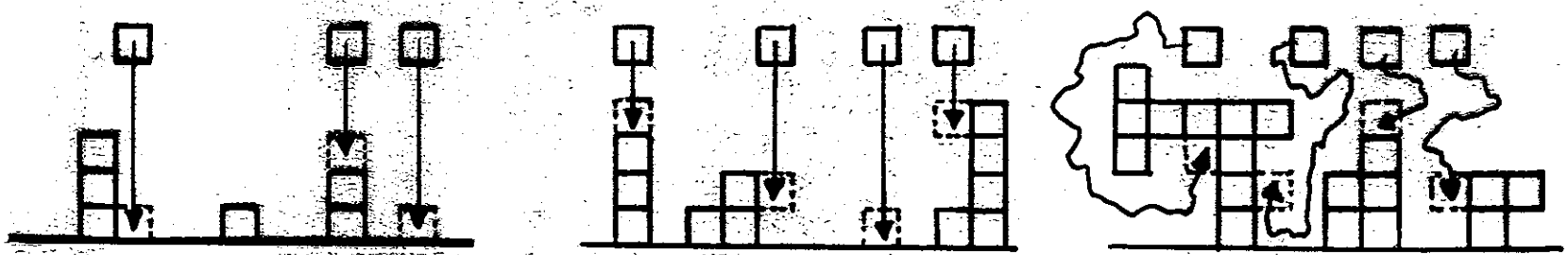

Random **D**ep. Ballistic Dep. Diffusion Limited **A**.

- A large family obeys **S**olid-**O**n-**S**olid restriction
- Cellular Automata / **M**onte **C**arlo rules

Discrete Gaussian Model:

See: Weeks & Gilmer
Adv. Chem. Phys. 40, 157 (1979)

$$H = \sum_{\substack{\text{nearest} \\ \text{neighbors}}} (h_i - h_{i+\delta})^2$$

La transición de "roughening"

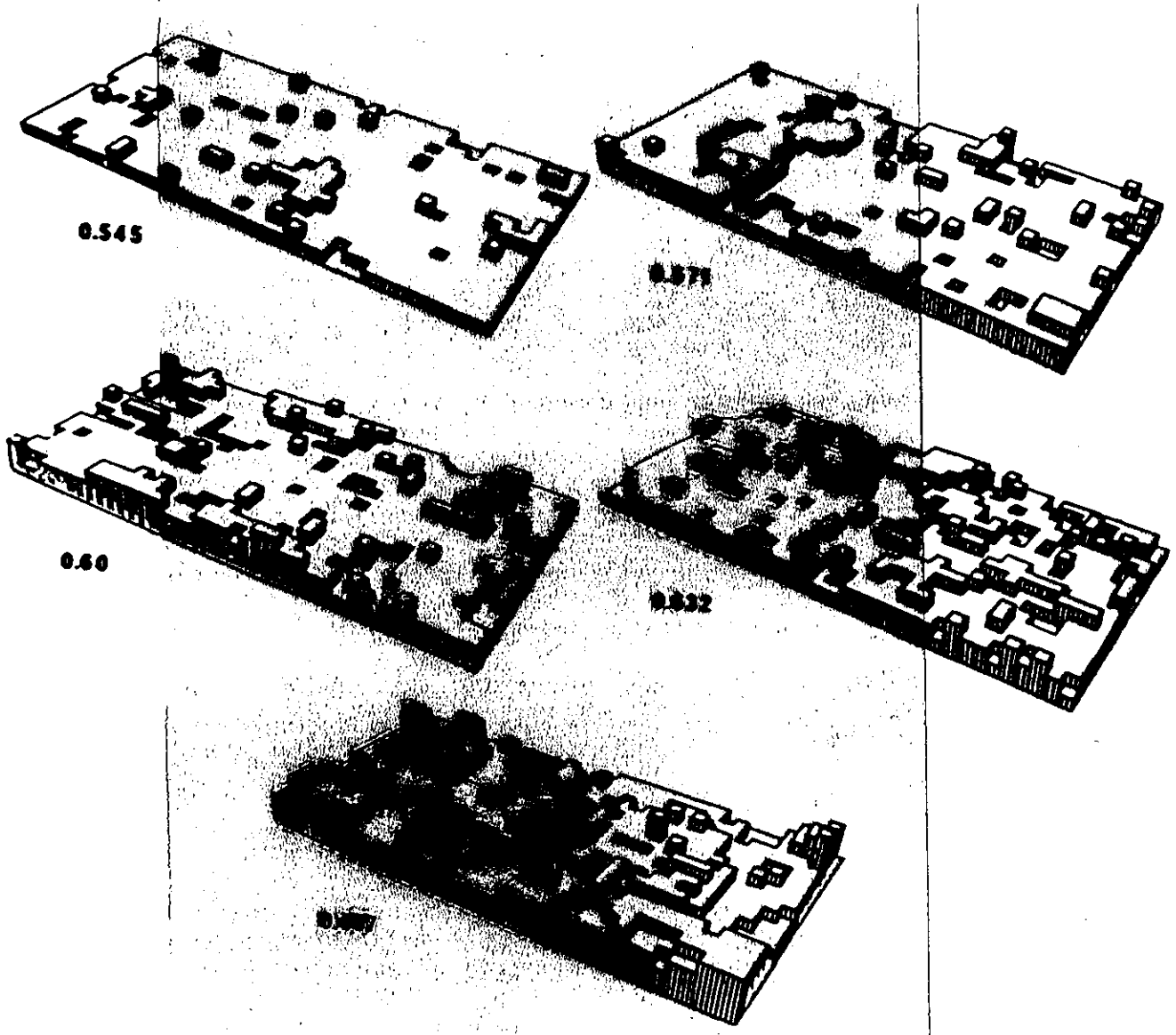

Fig. 10. Computer drawings of typical surfaces generated by the MC method at the indicated values of kT/ϕ.

Simulación Monte Carlo
(first predicted by Burton, Cabrera, & Frank)
3D vs Layer-by-Layer growth

Equilibrium Roughening

- Discrete Gaussian maps to Coulomb Gas:
  Roughening in the Kosterlitz-Thouless class — See Chui & Weeks (19… Phys. Rev. B 14, 49…
- Caracterization thru correlations

  $C(r) = \langle [h(R+r) - h(R)]^2 \rangle$

  ξ finite for $T < T_R$, $\xi = \infty$ for $T > T_R$

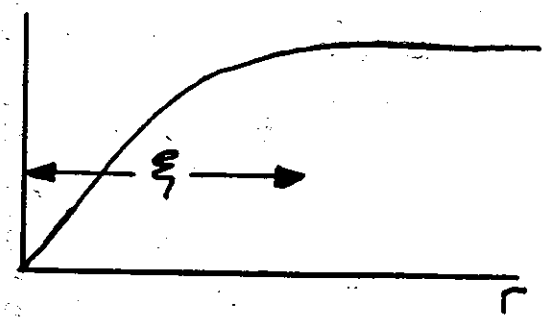

- Step creation energy vanishes at T_R
- Related results
  - Body Centered SOS: exact — van Beijeren, Phys. Rev. Lett. 38, 933 (1977)
  - Rigorous about SOS — Fröhlich & Spencer, Comm. Math. Phys. 81, 527 (1981)
- Experimental evidence in several systems

(Two-dimensional) sine-Gordon model

- Discrete Gaussian $\sum_{n.n.} (h_i - h_{i+\delta})^2$, $h_i \in \mathbb{Z}$ is modified to sine-Gordon $\sum_{n.n.} (h_i - h_{i+\delta})^2 - \sum_{sites} \cos h_i$, $h_i \in \mathbb{R}$ (discrete in space)

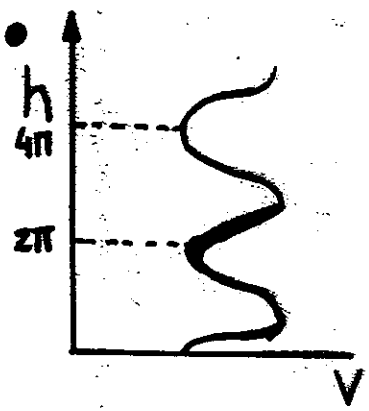

cos term favors $h \sim 2n\pi$,
roughening transition preserved
(renormalization group theory)

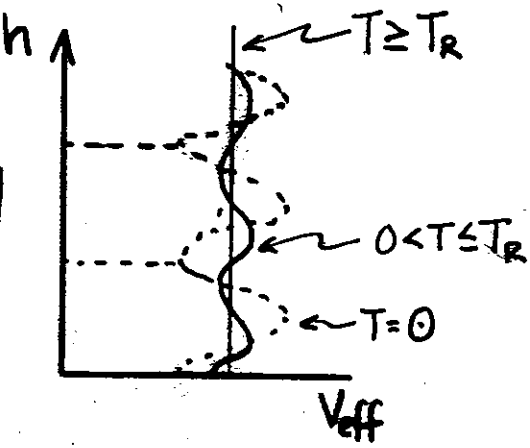

- Dissipative Dynamics

$$\dot{h}_i = \sum_{nn} (h_i - h_{i+\delta}) + \sin h_i + I + \xi_i(t)$$

I: average vapor chemical potential / overcooling / saturation

ξ_i: Gaussian white noise, $\langle \xi_i \rangle = 0$, $\langle \xi_i \xi_j \rangle = 2T\delta_{ij}\,\delta(t-t')$

- Langevin molecular dynamics $T_R \sim 2.5$ at $I = 0$ (equilibrium)

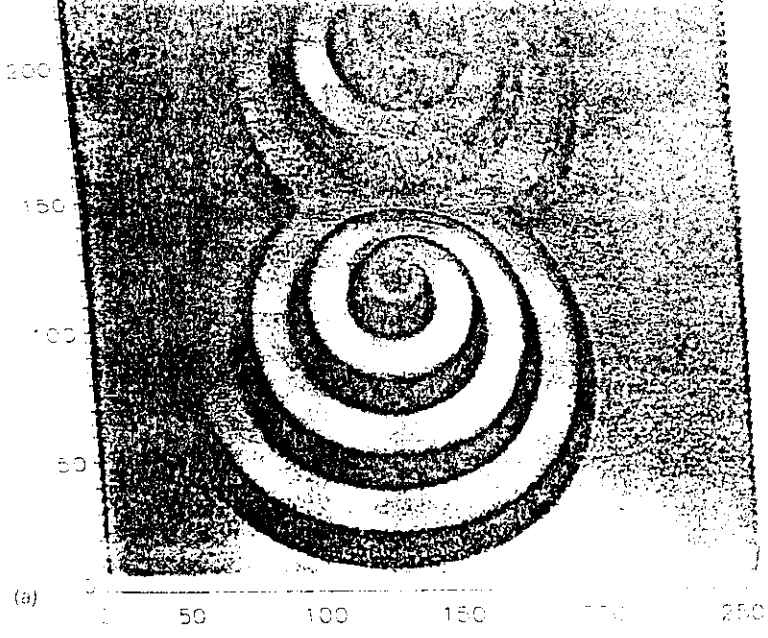

Model: Simulation (T≈0)

F. Fab, A.R. Bishop, P.S. Lomdahl, B. Horovitz (PRB 1991)

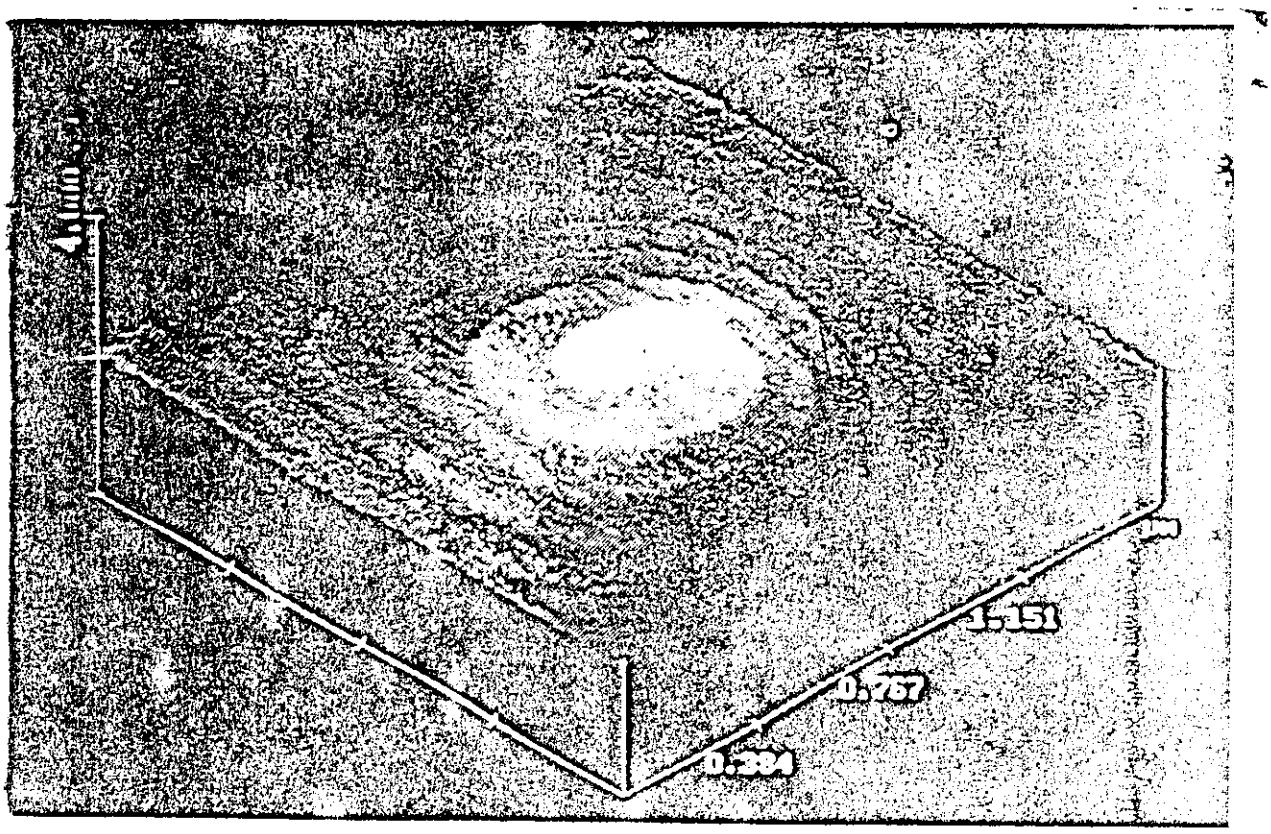

2. AFM image (1.5 μm×1.5 μm) of GaAs growth spiral pattern. e width is around 150 nm and step height is 0.28 nm. Epitaxial layer rown on small area (0.5 mm×0.5 mm) mesas in the same growth run Fig. 1. It clearly demonstrates the difference in the growth mechanism erent substrates under the same growth conditions.

C.C. Hsu, Y.C. Lu, J.B. Xu, I.H. Wilson (Appl. Phys. Lett. 1995)

b) Phase Diagram

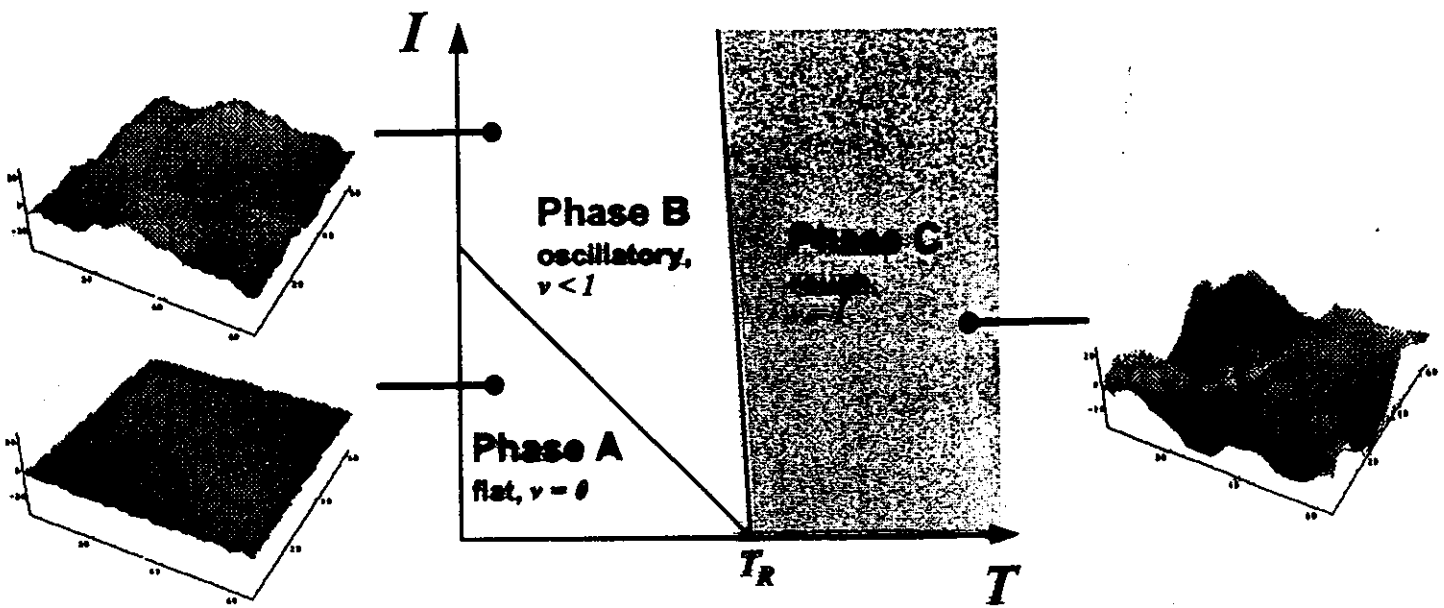

$$h(t) = \frac{1}{S}\int_S h(\vec{x},t)\,d^2\vec{x} = \begin{cases} const. & \text{Phase A} \\ \mu t \ (\mu < I) & \text{Phase B} \\ I\,t & \text{Phase C} \end{cases}$$

$$W^2(t) = \frac{1}{S}\int_S (h(\vec{x},t) - h(t))^2\,d^2\vec{x} = \begin{cases} const. & \text{Phase A} \\ oscillates & \text{Phase B} \\ \alpha S & \text{Phase C} \end{cases}$$

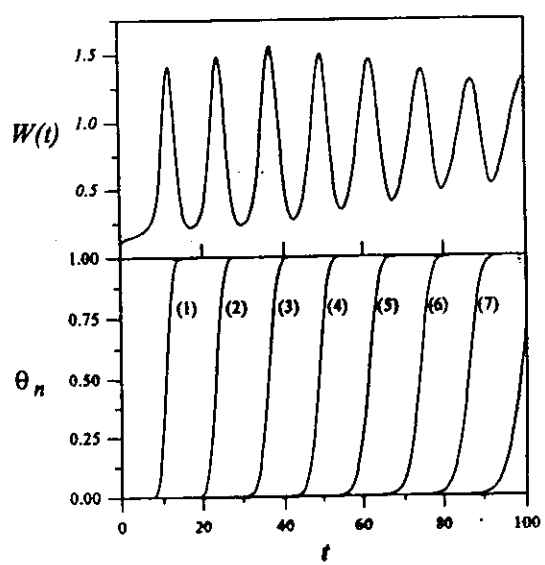

b) Approximations

$$\frac{\partial h(\vec{x},t)}{\partial t} = -\kappa \nabla^2\left(\nabla^2 h(\vec{x},t)\right) - V_0 \sin 2\pi \frac{h(\vec{x},t)}{a} + I + \eta(\vec{x},t)$$

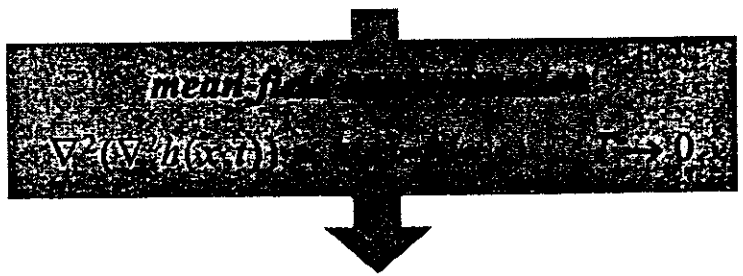

$$\frac{\partial h(\vec{x},t)}{\partial t} = \kappa\left[\bar{h}(t) - h(\vec{x},t)\right] - V_0 \sin 2\pi \frac{h(\vec{x},t)}{a} + I + \eta(\vec{x},t)$$

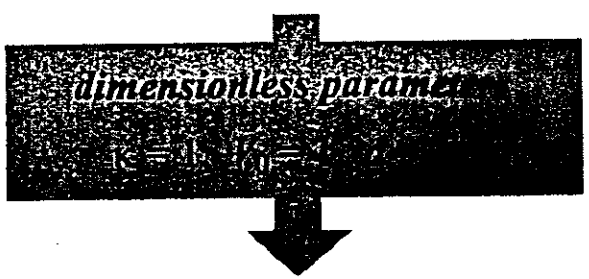

$$\frac{\partial h(\vec{x},t)}{\partial t} = \bar{h}(t) - h(\vec{x},t) - \sin h(\vec{x},t) + I + \sqrt{2T}\,\xi(\vec{x},t)$$

2. Perturbative Analysis $2T = \varepsilon \to 0$

Two ways:

Stochastic Model

Fokker-Planck Eq.	**Stochastic Differential Eq.**
$\frac{\partial p(h,t)}{\partial t} = \frac{\varepsilon^2}{2}\frac{\partial^2 p(h,t)}{\partial h^2} - \frac{\partial}{\partial h}\left\{ \overline{h}(t) - h - \sin h + I \; p(h,t)\right\}$	$\frac{\partial h}{\partial t} = \overline{h}(t) - h - \sin h + I + \eta(t)$
$\overline{h}(t) = \int_{-\infty}^{\infty} h\, p(h,t)\, dh$	$\frac{\partial \overline{h}(t)}{\partial t} = -\sin h + I$
$p(h,t) = p_0(h,t) + \varepsilon\, p_1(h,t) + \varepsilon^2 p_2(h,t) + \cdots$	$h(t) = h_0(t) + \varepsilon\, h_1(t) + \varepsilon^2 h_2(t) + \cdots$
Singular Problem WKB Methods	**Not a Singular** Problem Simple Perturbation analysis
Not a probabilistic expansion **Difficult** to obtain even the **first order**	**Itô** or **Stratonovich** Calculus Easy to see **other singular** effects

3. Application to our Model

• We will study the oscillations for $I >> 1$ (if $I = 1 + a\varepsilon + O(\varepsilon^2)$ the calculations more complicated)

• Inserting the ansatz in the mean field equation:

$$h(t) = h_0(t) + \varepsilon h_1(t) + \varepsilon^2 h_2(t) + \cdots$$

and equating coefficients of like powers of ε:

$$O(0) \qquad \frac{\partial h_0}{\partial t} = \bar{h}_0 - h_0 - \sin h_0 + I$$

$$O(\varepsilon) \qquad \frac{\partial h_1}{\partial t} = \bar{h}_1 - h_1 - h_1 \cos h_0 + \eta(t)$$

$$O(\varepsilon^2) \qquad \frac{\partial h_2}{\partial t} = \bar{h}_2 - h_2 - h_2 \cos h_0 - \frac{h_1^2}{2} \sin h_0$$

• We are interested in the mean value and roughness:

$$\bar{h}(t) = \bar{h}_0 + \varepsilon \bar{h}_1 + \varepsilon^2 \bar{h}_1 + \cdots$$

$$W^2(t) = \varepsilon^2 \overline{h_1^2} + \cdots$$

Order	*Mean value*	*Variance*	*Plot*
$O(0)$	$\frac{\partial \overline{h_0}}{\partial t} = I - \sin \overline{h_0}$	$\overline{h_0^2} = \left(\overline{h_0}\right)^2$	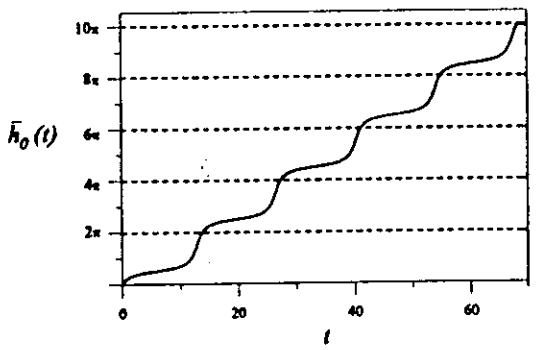
$O(\varepsilon)$	$\overline{h_1}(t) = 0$	$\frac{\partial \overline{h_1^2}}{\partial t} = 1 - 2(\overline{1} + \cos \overline{h_0})\overline{h_1^2}$	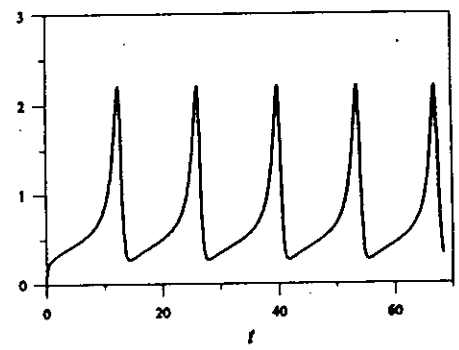
$O(\varepsilon^2)$	$\frac{\partial \overline{h_2}}{\partial t} = \frac{\overline{h_1^2}}{2} \sin \overline{h_0} - \overline{h_2} \cos \overline{h_0}$	—	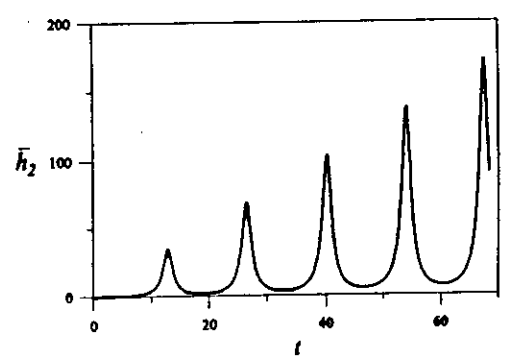

(• The period of the oscillations is $P = \frac{2\pi}{I^2 - 1}$)

- Our ansatz does not work because we need to take into account another time scale:

$$\underbrace{\frac{\partial h}{\partial t} = a(h,t) + \varepsilon\eta(t)}_{\text{time scale} = t} \qquad \frac{\partial h}{\partial t} = \overbrace{a(h,t) + \varepsilon\eta(t)}^{\text{time scale } \tau = \varepsilon^2 t}$$

Then the ***noise provides another time scale.***

- We apply ***Lindstedt's method*** to deal with t and τ

$$t^* = t(1 + \alpha\varepsilon^2 + O(\varepsilon^3)) \Rightarrow$$

$$\frac{\partial \bar{h}_0}{\partial t^*} = I - \sin\bar{h}_0$$

$$\frac{\partial \bar{h}_1^2}{\partial t^*} = 1 - 2(1 + \cos\bar{h}_0)\bar{h}_1^2$$

$$\frac{\partial \bar{h}_2}{\partial t^*} = \left(\frac{\bar{h}_1^2}{2} + \alpha\right)\sin\bar{h}_0 - \alpha I - \bar{h}_2\cos\bar{h}_0$$

- To calculate α we apply the solvability condition to the third equation

> if $y(t^*)$ is solution of $Ly(t^*) = 0$, **where** $Ly = \frac{\partial y}{\partial t^*} + y\cos h_0 \Rightarrow y \perp g$

$$g(t^*) = \sin\bar{h}_0\left(\frac{\bar{h}_1^2}{2} + \alpha\right) - \alpha I$$

• Thus

$$\alpha = \frac{1}{P^*}\int_0^{P^*} \frac{\overline{h_1^2}}{2}\,\frac{\sin\bar{h}_0}{I-\sin\bar{h}_0}\,dt^* \qquad P^* = \frac{2\pi}{I^2-1}$$

In the former time scale t, the period of the oscillations is equal to:

$$P = \frac{P^*}{1+\alpha(I)\varepsilon^2+O(\varepsilon^3)} = \frac{2\pi}{I^2-1}\,\frac{1}{1+\alpha(I)\varepsilon^2+O(\varepsilon^3)}$$

The period of the oscillations depends on the (ε) temperature!!!

• Comparison with numerical simulations